Characterization of Al^{+3} Substituted Sr Nano-Hexaferrite Synthesised by Sol-Gel Auto Combustion Technique.

A.S.Kakde*, A. D. Deshpande^, S. D. Chachere#, M. S. Choukuse%, D. V. Nandanwar!, P.S.Sawadh@ , K.G.Rewatkar*

*Department of Physics, Dr. Ambedkar College, Nagpur-10
^Department of Physics, Priyadarshini College of Engg., Napur.
#Department of Chemistry, Shri Dynanesh Mahavidyalaya, Nawargaon.
% Department of Applied Physics, Govt. of Engg. College, Phonda, Gao
! Department of Physics, M.M. College of Science, Nagpur.
@Department of Physics, Bapurao Deshmukh College of Engg. Sewagram, Wardha
Corresponding author email: anandkakde85@gmail.com

Abstract:

Single phase nano-crystalline particles of strontium hexaferrite have been pleasingly synthesized in one step via a microwave-assisted sol–gel auto-combustion route. The characterization consequences of the research module reveal that synthesized product may have potential applications in the area of magnetic data storage and high-frequency devices. The crystal structure remains unaltered by the Al^{+3} substitutions. The crystallite size in the range of 14-42 nm is determined from the X-ray diffraction. Scanning electron micrographs of the samples showed homogenous microstructures. The magnetic properties such as saturation magnetization, remanence and coercivity are calculated from the hysteresis loops. The values of saturation magnetization are found to be increase while that of remanence and coercivity showing decreasing trend.

Keywords: nano-crystalline, XRD, saturation magnetization, remanence, coercivity etc.

1.   Introduction

M-type hexagonal ferrites having the general formula $MFe_{12}O_{19}$(where M is Sr, Ba or Pb) are hard magnetic materials with a magnetoplumbite structure. M-type hexagonal ferrites are still of enormous technical importance in the permanent magnet market because of their low price and reasonable magnetic properties. Moreover, the hexaferrite nanoparticles have recently attracted much attention due to their potential in micro-electro mechanical systems (MEMS) and biomedical applications [1, 2]. In such a context, improvement of their hard magnetic properties is of great importance. Because of the fact, that strontium ferrite has a low price per unit available magnetic energy, this material continues to occupy an importance particular in the permanent magnets market. This material is chemically stable and once known for its high uniaxial magnetocrystalline anisotropy with an easy axis of magnetization along the hexagonal c-axis [3,4]. The magnetic properties of anisotropic M-type $SrFe_{12}O_{19}$

hexagonal ferrites can be improved by applying Al^{+3} substitutions [5]. With the substitution of Al^{+3} for Fe^{+3}, the saturation magnetization, coercivity, anisotropy constant and ferromagnetic resonant frequency of strontium ferrite is changed. In the present research module, the effect of calcination temperature with respect to Al^{+3} concentrations on the structures and the magnetic properties of synthesised samples studied systematically.

2.   Experimental

The Al substituted strontium ferrite particles were prepared using sol-gel auto combustion method [6]. According to the composition of $SrAl_xFe_{12-x}O_{19}$ (x = 0, 0.5)stoichiometric amount $Sr(NO_3)_2$, $Fe(NO_3)_39H_2O$, $Al(NO_3)_39H_2O$ were dissolved in deionized water followed by the subsequent addition of urea [7]. An ammonia solution was added to adjust the pH value to 7.0. The solution was slowly evaporated at 80 ^{0}C until a viscous gel formed. The dried gel then was put in the specially designed microwave oven, where gel get burnt by self propagating combustion reaction evolving large volumes of gases and finally gets converted in ash brown powder. The ash brown powder of samples was crushed in the pestal mortar to have ultrafine strontium hexaferrites powder. The synthesized sample was calcined at 800 ^{0}C for about 4 hours in the electric furnace to obtain monophase M-type strontium hexaferrites.

The crystalline structure of strontium ferrite powder was investigated with X-ray diffraction (XRD). XRD analysis was performed on a Bruker-AXS advanced diffractometer with Cu Ka radiation in the 2θ range from $10^θ$ to $80^θ$ by steps of 0.021 with λ = 1.5405 Å. Scanning electron micrograph (SEM) was recorded on SEM-JSM-7600F. The saturation magnetization and coercivity of the strontium ferrite powder was measured by means of vibrating sample magnetometer (Lakeshore VSM 7410) at a maximum applied field of 15,000 Gauss at room temperature.

3.   Results and Discussion

Fig. 1 shows the XRD patterns of $SrAl_xFe_{12-x}O_{19}$ of the as sintered samples. It is clear from the pattern that all samples are in single phase **(JCPDS# 080-1197)** with hexagonal structure without showing any detectable impurities and there no unreacted constituents are present in these samples.
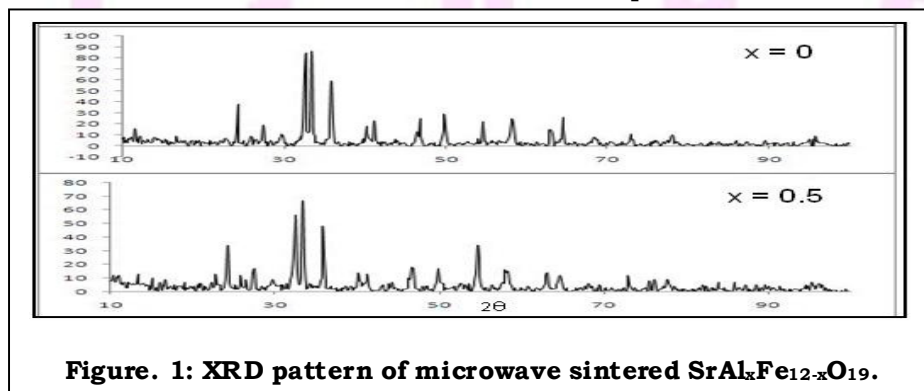

Figure. 1: XRD pattern of microwave sintered $SrAl_xFe_{12-x}O_{19}$.

Table 1: X-Ray Diffraction Calculations for the samples SrAl$_x$Fe$_{12-x}$O$_{19}$

Conc. (x)	Lattice Parameters		c/a (Å)	X Ray Density (gm/cm³)	Bulk Density (gm/cm³)	Porosity (%)	Particle Size (nm)
	a (Å)	c (Å)					
x = 0	5.8000	22.3626	3.85	5.7105	2.6367	53.82	26
x = 0.5	5.9486	22.0848	3.71	5.4235	2.5427	53.12	64

From structural parameters characterized by lattice constants 'a' and 'c' (Table 1) shows slight variation with substitution of Al^{3+} ions. This is in agreement with the fact that all hexagonal ferrite exhibits constant lattice parameter 'a' variable 'c'. It also indicates that change of easy magnetized c-axis is larger than a-axis with Al^{3+} ions substitution [8].It is obvious that as Fe^{3+} (0.67 Å) has larger ionic radii than Al^{3+} (0.50 Å) and hence 'a' is predominantly governed by large Fe^{3+} ions. The Al^{3+} causes compressive strain in the lattice due to its smaller ionic radii and therefore gives rise to shrinkage of the crystal [9]. The crystallite size of Sr-ferrite present in the investigated solids was based on X-ray diffraction line broadening and calculated by using Scherrer equation [10]. The crystallite size was to be found in the nanometer range as depicted in table 1.
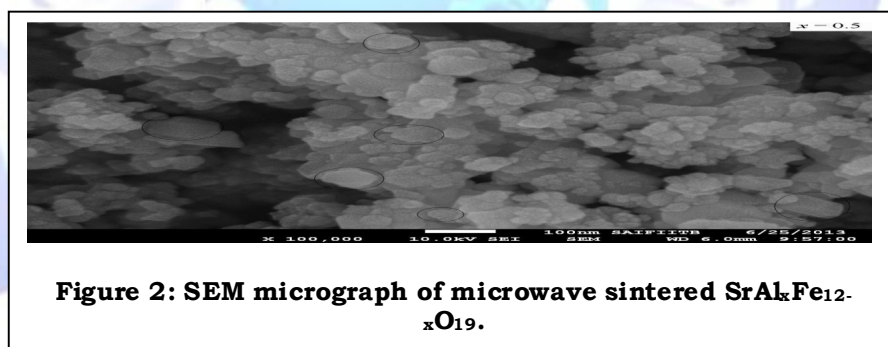

Figure 2: SEM micrograph of microwave sintered SrAl$_x$Fe$_{12-x}$O$_{19}$.

The HR-SEM micrograph for the microwave calcined powder at 800°C for 4 hrs is shown in Figure 2. The particles are like hexagonal platelets and have well defined crystalline behavior with diameters are in the range of 26 nm to 64 nm. This type of shape is usually observed for SrFe$_{12}$O$_{19}$ obtained by sol-gel process [11, 12]. The morphology of the microwave calcined powder samples reveal smaller particles size compared to the conventionally calcined powder and its influence on magnetic properties are discussed in the subsequent sections.

Figure 3: Hysteresis loop of microwave sintered $SrAl_xFe_{12-x}O_{19}$.
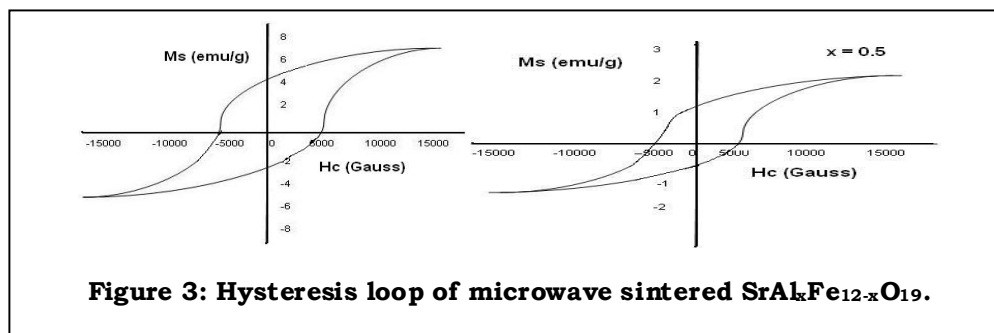
It has been observed from the table 2 that the saturation magnetization, retentivity and coercivity decrease with increase in the substitution of Al^{3+} ions in SrM hexaferrite. The substituent Al^{3+} ions preferred to enter in the 12k (octahedral) site which has spin in upward direction. The replacement of Fe^{3+} by the nonmagnetic ions from the site of upward spin reduce the number of electrons with upward spin and result in decreasing the net magnetic moment as well as the saturation magnetization and remanence [13, 14]. The decrease in coercivity for the Al^{3+} ion doped samples is due to the replacement of iron ions from 12k site to results in a reduction in the magnetocrystalline anisotropy. This consequently decreases the coercivity for the samples of SrM hexaferrite [15]. The coercivity has a great dependence on grain size, with the increasing Al^{+3} concentration the surface to volume ratio decreases as the grain size increases by falling the coercivity [16]. This fall of coercivity causes the change from hard ferrites to soft ferrites. Decrease in the magnetization of the synthesized hexaferrites together with the decrease in the coercivity of the Al^{+3} ions doped strontium hexaferrites validates their possible use in magnetic data storage devices.

Table 2: VSM Calculations for $SrAl_xFe_{12-x}O_{19}$

Conc. (x)	Saturation Magnetization (emu/g)	Retentivity (emu/g)	Coercivity (Gauss)
x = 0	7.2300	13.1370	6130
x = 0.5	2.1540	3.6500	4230

4. Conclusion

Remarkable changes in microstructure and magnetic properties (M_s and H_c) were obtained by the substituent. A simple and economical route has been presented for producing homogeneous Al^{+3} ions doped Sr-hexaferrite by the sol-gel auto combustion method subsequently at low sintered temperature of 800°C to acquired single phase $SrFe_{12-x}O_{19}$ nano-powder. The substitution of Al^{+3} ions causes grain coarsening and more expansion of crystal lattice towards c-axis than a-axis. The

scanning electron microscopy reveals that as Al^{+3} ions concentration increases the average grain size increases. The change in magnetic parameters results in possible use of substituted ferrite for permanent magnet at low level substitution.

References

1. S. Mornet, S. Vasseur, F. Grasset and E. Duguet, J.Mater. Chem. 14, 2161 (2004).

2. T. T. V. Nga,_ T. D. Hien, N. P. Duong and T. D. Hoang, Journal of the Korean Physical Society, Vol. 52, No. 5, , pp. 1474_1477 (2008).

3. J. Smit and H.P.J. Wijn, (Eindhoven: N.V. Philips Gloeilampenfabrickon, 1959).

4. Anterpreet Singh, S. BindraNarang, Kulwant Singh, O.P. Pandeyand R.K. KotnalaJournal of Ceramic Processing Research. Vol. 11, No. 2, pp. 241~249 (2010)

5. S. A. PAWADE, K. G. REWATKAR, V. M. NANOTI, International Journal of Knowledge Engineering, Volume 3, Issue 1, 2012, pp.-31-35.

6. Sharad N. Sable, Sanjay R. Gawali, Kishor G. Rewatkar, Vivek M. Nanoti; Bionano Frontier, Vol. 5) 460–463, (2012).

7. Asmita Deshpande, Sharad N. Sable, Vivek M. Nanoti, Kishor G. Rewatkar; NANOTRENDS 2009–10 (In Modern Technoscientific Era) pp 26–27, 2010.

8. Q Jianxun, G Mingyuan, S Haigen, J. of Magn. and Mag. Materials, 295, 263–268, (2005).

9. S. A. Pawade, V. K. Nanoti, S. D. Kulkarni, K. G. Rewatkar, J. Bionano Frontier, issue 5, 2012. P 93-99. 21, (2012).

10. B.D. Cullity, Elements of X-ray Diffraction, Addison-Wesly Publishing Co. Inc. (1976)

11. H. Shang, J. Wang and Q. F. Liu, Materials Science and Engineer-ing: A, Vol. 456, No. 15, pp. 130-132 (2007).

12. R. M. Garcia, E. R. Ruiz and E. E. Rams, Materials Letters, Vol. 50, No. 2-3, , pp. 183-187, (2001).

13. Fang Q. Q., Cheng, H., Huang K., Wang J., Li R., Jiao Y., J. Magn. Magn. Mater. 294, 281, (2005).

14. Singhal S., Garg A. N., Chandra K., J. Magn. Magn. Mater. 285 193(2005).

15. Y. Topal, H. Ozkan, H. Sozeri, *J. Mags& Mag. Mat.,284*, 416-422, (2004).

16. N. Rezlescu and E. Cuciureanu, *Phys. Stat. Sol.,***3**, 873, (1970).